DOI: 10.1021/ma1007732

Macromolecules
ARTICLE

Fabrication of Morphology-Controlled Sub-20-nm Polymer Nanotip and Nanopore Arrays Using an Identical Nanograss Mold

Chien-Chong Hong,*,† Pin Huang,† and Jiann Shieh‡

†*Department of Power Mechanical Engineering, National Tsing Hua University, Taiwan, and*
‡*National Nano Device Laboratories, Hsinchu, Taiwan*

Received April 14, 2010; Revised Manuscript Received July 31, 2010

ABSTRACT: This paper presents the fabrication of morphology-controlled sub-20-nm polymer nanotip and nanopore arrays using an identical nanograss mold. Cyclic olefin copolymer (COC) plastic surfaces with controllable nanostructural morphologies have been successfully nanoimprinted with different molding temperatures using the identical silicon master mold structure. Low-aspect-ratio sub-20-nm polymer nanopore and nanotip arrays can be fabricated at molding temperatures below the glass temperature of COC plastic. And high-aspect-ratio sub-20-nm polymer nanotip and nanopore arrays can be fabricated at molding temperatures above the glass temperature of COC plastic. It shows that a COC plastic modified from the native contact angel of 90° into a hydrophobic and superhydrophobic surface with a maximum contact angel of 155° by only changing the surface morphologies. Depending on surface nanostructures, the optical transmittance of COC with nanoimprinted surfaces was changed ranging from 86% to 94%. The optical transmittance of the COC chip with double-sided nanostructured surfaces increased from 90% to 95%. The developed technique is simple, ease of fabrication and low cost to realize morphology-controlled sub-20-nm nanotip and nanopore arrays using the identical silicon mold structure. Sub-20-nm polymer nanostructures with different morphologies can be fabricated by varying molding temperatures.

Introduction

High aspect-ratio (HAR) structures, defined as heights to widths of structures larger than 10, have recently attracted great interest for scientists and engineers. These HAR structures in microscale have been developed and realized in most materials in recent years.[1,2] Biommetic nanoengineering has recently focused on and discovered several existing HAR nanostructures in nature. One example is the gecko's fingers, which use HAR nanostructures to exhibit strong adhesive force.[3] Nanostructures also change surface energy and optical properties, such as hydrophilicity, hydrophobicity and optical reflection, due to the features of HAR nanostructures. Because of progress on nanotechnology, it has recently become possible to make HAR structures in nano scale, such as nanotubes, nanowires, nanorods, nanotips, and nanopores. Most nanostructures are made of inorganic materials, such as silicon, glass, zinc oxide, and metals. Besides fabricating inorganic nanostructures in high aspect ratio, recent researches are focusing on HAR nanostructures of polymer materials. Researchers have successfully developed fabrication technologies for polymer HAR nanostructures with hundreds of nanometer features.[4−6] Recently, researches have focused on the feature size below 100 nm for polymers and the physical and chemical properties of developed novel polymer HAR nanostructures are still under investigation.

Past research literatures have found that HAR nanostructures improve performance on electric effects[7,8] and have studied HAR nanostructures to discover their electromagnetic effect for molecular sensing.[9] Recently, nanopores have been studied to discover their novel optical properties.[10] Nanostructures change optical properties and surface energy, such as optical reflection and hydrophobicity, due to the features of nanostructures. Superhydrophobocity, defined as the water contact angle in excess of 150°, plays an important role in the field of science and engineering, dominating several applications, such as microfluidics, protein absorption, cell culturing, and self-cleaning surface.[11−13]

Several previous techniques have been developed to realize superhydrophobicity on engineering materials by chemically modified silicon nanograss,[14] chemical coating on polymer surfaces,[15] or by plasma treatment of polymer surfaces.[16] The lotus leaf and rose petal are two examples in nature that exhibit superhydrophobicity.[17] Several biommetic designs following these features developed artificial lotus-like structures[18] or multiscale hybride micro/nanostructures.[19] Researchers have also applied several techniques to modify polymer substrates to superhydrophobic surfaces, such as elecrospun nanofiber coating[20] and chemically modified carbon nanotube forest.[21] However, these only retain superhydrophobicity, but lose optical transparency after surface modification. Superhydrphobicity and high transparency are very important for some applications in optics, biology, and energy. Only a few surface treatment techniques have created transparent and superhydrphobic surfaces together with silica-based thin film,[22] silica nanoparticles treatment,[23] and plasma etched HAR nanostructures with Teflon-like coating.[24] These surface coatings on polymer materials face problems of long-term stability. Past literatures demonstrate that 20 nm HAR silicon nanostructures on silicon wafers reduce optical reflection and enhance hydrophobicity greatly with CHF_3 coating.[25,26] In the past years, similar morphologies and length scales have been reported by several groups through the use of block copolymer self-assembly.[27−29] In addition, large-area sub-20-nm nanopillar arrays and nanohole arrays have been realized on SiO_2 by nanolithography.[30] The polymer nanotips or nanopores have been realized using negative master molds or positive master molds, respectively. However, studies to date have not realized or investigated HAR polymer nanotip and nanopore arrays at 20 nm scale using the identical positive master mold only.

*Corresponding author. Mailing address: 101, Sec. 2, Kuang Fu Rd., Engineering Building I, Room 629, Hsinchu, Taiwan. E-mail: cchong@mx.nthu.edu.tw. Telephone: 886-3-5715131-33736. Fax: 886-3-5722840.

 Published on Web 08/17/2010

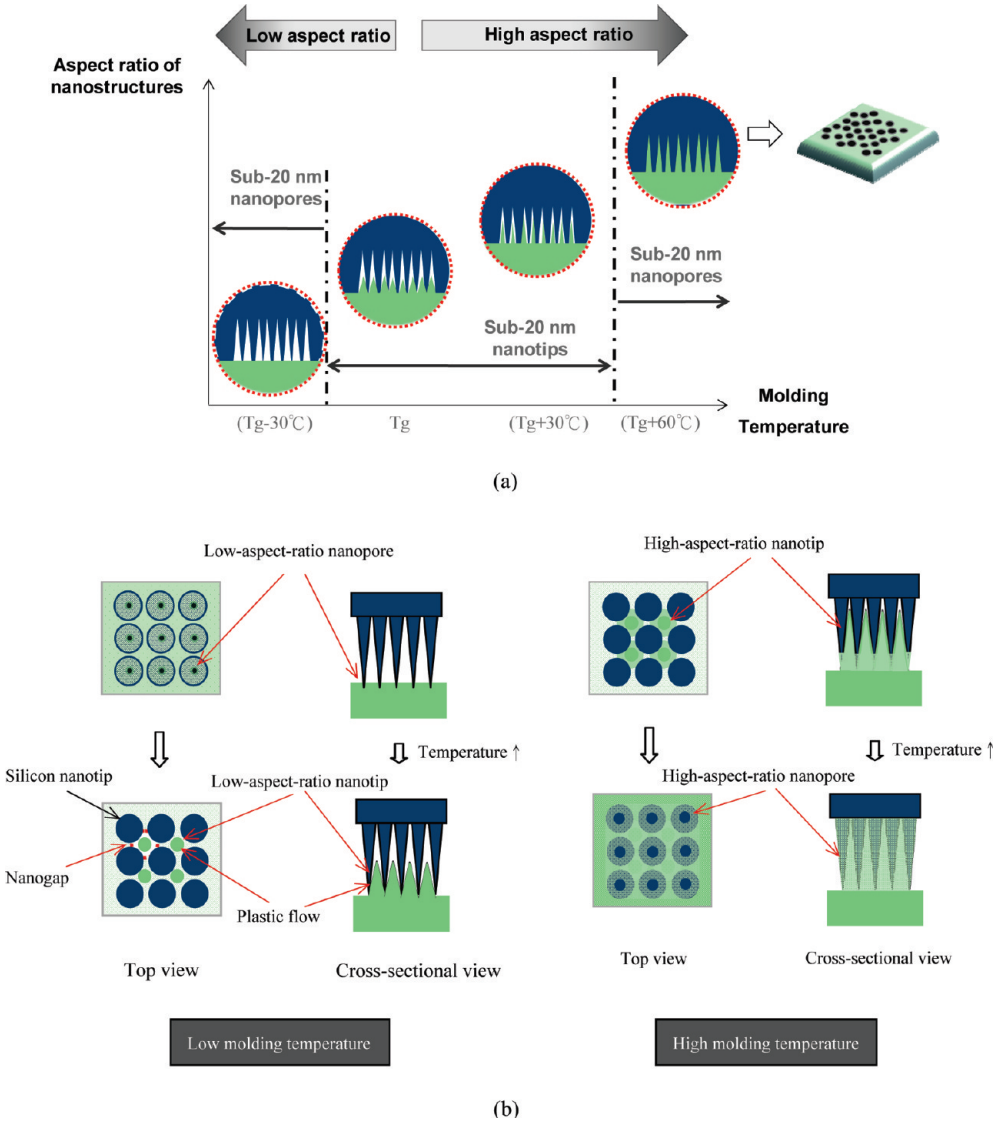

Figure 1. Schematic illustration of the morphology-controlled sub-20-nm polymer nanotip and nanopore arrays by thermal nanoimprinting with different molding temperatures; (a) The relationship between nanostructural morphologies and molding temperature and (b) filling of molding plastic flow among the nanogaps to form nanotip and nanopore arrays under different molding conditions.

Nanoimprint lithography (NIL) is one of the most promising nanofabrication technologies for mass production in the nanoscale. NIL is often used to replica the inverse patterns of the original master structures. Up to date, although several researches has successfully achieved nanostructures under 20 nm using nanoimprinting lithography (NIL),[31,32] there is no research realizing and studying HAR nanostructures under 20 nm. In this paper, HAR nanotips and nanopores less than 20 nm using the identical mold structure by thermal NIL have been first studies. The study in this paper applied thermal NIL to realize not only the inverse patterns of the original master structures, but also the positive patterns using the identical master mold structures. Different morphologies of sub-20-nm polymer nanostructures can be made by the developed techniques with the identical sub-20-nm silicon master mold structure. Low-aspect-ratio (LAR) nanopore arrays can be fabricated at the temperature below the glass temperature of the polymer materials. As the molding temperature is increased, LAR nanotip arrays can be fabricated. As the molding temperature is set higher, HAR polymer nanotip arrays with different aspect ratios can be fabricated using the silicon nanograss mold structures by adjusting one of nanoimprinting process parameters. While the molding temperature is set higher than the glass temperature of the polymer materials, HAR nanopore arrays are formed instead of nanotip arrays.

In BioMEMS applications, cyclic olefin copolymer (COC) is one of the most popular choices for substrate material because of its excellent molding, biomedical, and optical properties. Researches often apply plasma processing for surface modification of COC plastic surfaces. Plasma-treated surface modification probably has a problem with long-term stability. This work first develops a novel and simple technique to make a COC plastic surface with sub-20-nm HAR nanostructures. In addition, morphology-controlled techniques of sub-20-nm polymer nanotip and nanopore arrays are developed using the identical silicon mold structure. Studies have investigated further development of nanotip and nanopore arrays with different morphologies on COC plastic by varying the nanoimprinting process. This paper also characterizes surface and optical properties of the nanoimprinted structures.

The current work creates morphology-controlled sub-20-nm polymer nanotips and nanopores by changing the temperature of the nanoimprinting process. First, during thermal nanoimprinting, these minute nanoscale cavities can only be filled to a certain degree due to limitations in the polymer's surface energy, molecular weight

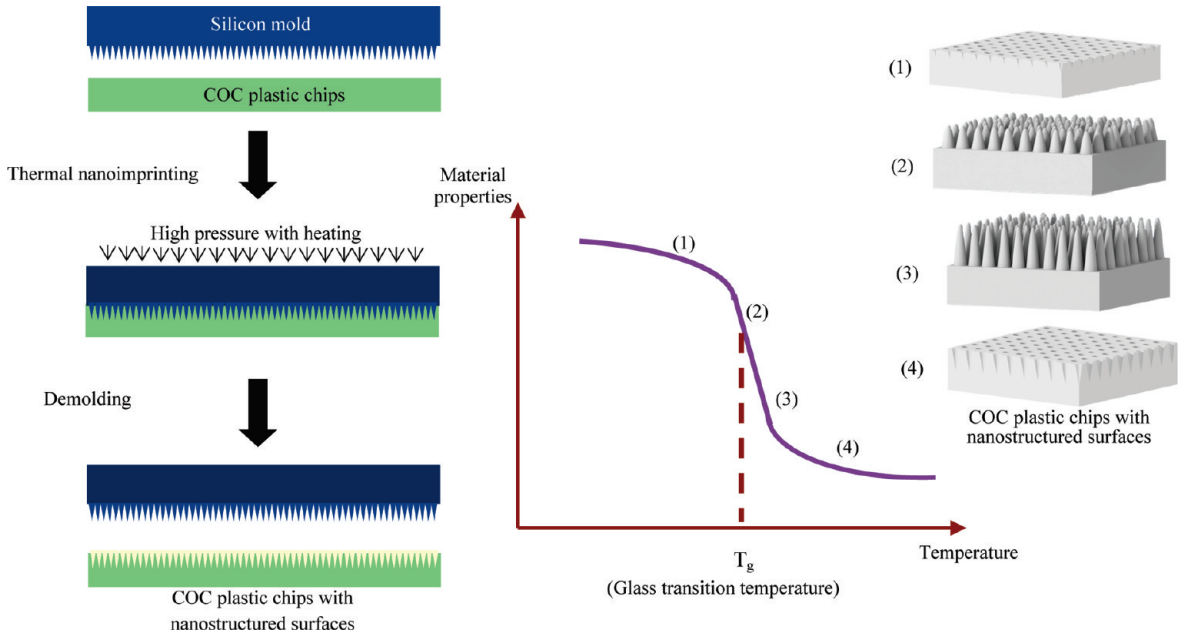

Figure 2. Schematic drawing of the fabrication process to realize sub-20-nm nanotip and nanopore arrays on polymer surfaces.

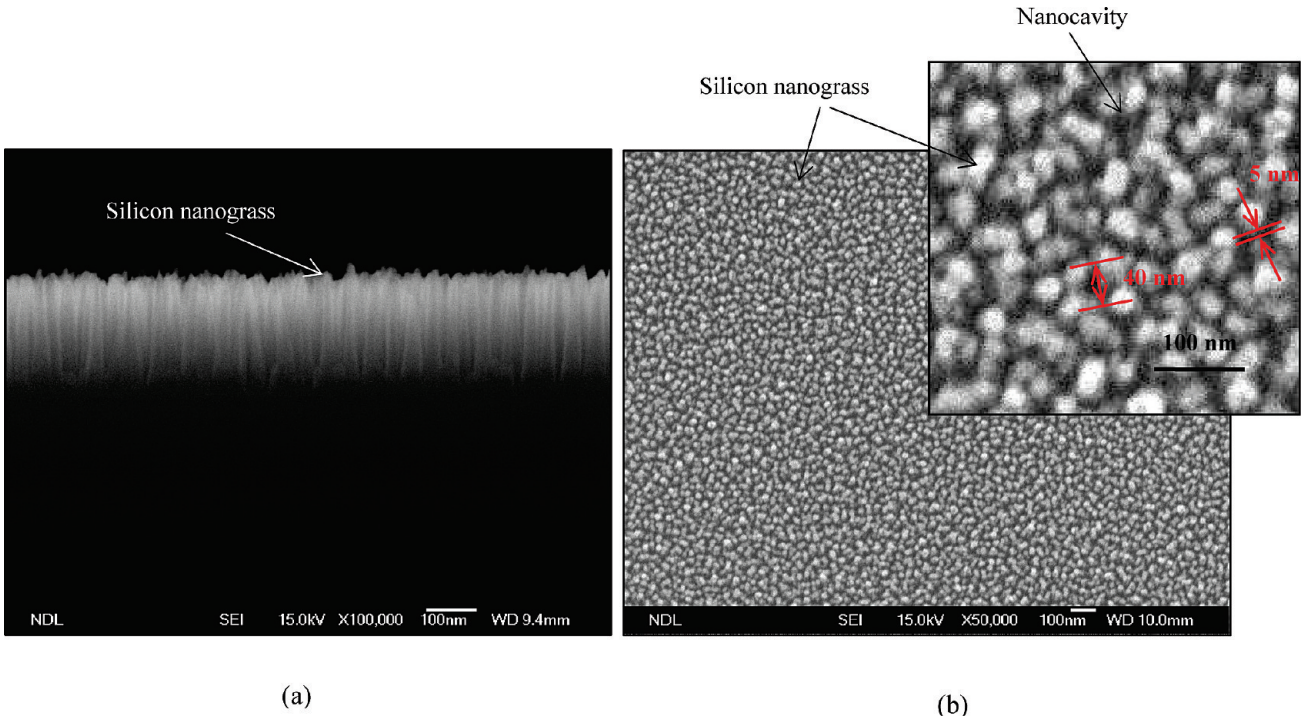

Figure 3. SEM pictures of the Si nanograss master mold: (a) the side view and (b) the top view. The inset image is the top view with high magnification.

and other physical properties such as plastic flow rate. Second, antisticking treatment is generally by way of coating a release agent, but as the sizes become smaller, the contact area becomes larger, which means these large numbers of molecules produce adhesion similar to the gecko effect which determines the degree of difficulty in demolding. This work investigates the replicated morphologies and surface characteristics by changing the temperature of the nanoimprinting process, making the nanostructure of nanotip and nanopore arrays using COC polymer materials. Because the viscosity coefficient of polymer material is extremely volatile to temperature changes near its glass temperature, different process temperatures lead to different velocities of plastic flow in the mold cavities, thereby affecting the degree to which nanoscale cavities are filled. As described in Figure 1, this work develops a novel and simple technique to make morphology-controlled sub-20-nm COC polymer nanotip and nanopore arrays by thermal nanoimprinting with different molding temperatures. The polymer surface is heated to be softened while it is heated up to the specific temperature, so the silicon nanotips slightly penetrate into the polymer surface to form low-aspect-ratio nanopore arrays at low molding temperatures. As the molding temperature is increased, the plastic flow starts to fill the nanogap among four nanotips to form low-aspect-ratio polymer nanotip arrays. The plastic flow tends to enter the larger nanogaps and not to fill the small nanogaps due to the very high flow resistance in the small nanogap arrays. So, high-aspect-ratio nanotips are formed at this stage. Finally, when the plastic

flow reaches near the bottom of nanogap, which is less than 5 nm, it requires higher temperature to further reduce viscosity of plastic flow and fill all the small nanogaps to form high-aspect-ratio nanopore arrays.

Fabrication Process

Figure 2 shows a schematic drawing of the fabrication process to realize sub-20-nm nanotips/nanopores on polymer surfaces. A silicon mold was used to nanoimprint nanostructures on a COC wafer. This research uses a well-aligned silicon nanograss of sub-20-nm with high-aspect-ratio, fabricated on a 6-in. silicon wafer through hydrogen plasma etching alone, as a thermal nanoimprinting mold. The silicon nanograss master mold was fabricated in single step through hydrogen plasma etching without any mask or catalyst. The 6 in. silicon ⟨100⟩ wafer was placed in the plasma chamber and then was heated to 400 °C before introducing hydrogen gas at a rate of 200 sccm. The 500 W RF and 300 kHz bias powers were turned on to start the plasma etching. The morphologies and aspect ratio of nanograss structures can be changed by adjusting the duration of the plasma process. The procedure of creating silicon master molds has been published in a previous paper by our coauthor, J. Shieh.[33] In this work, the silicon wafer was etched for 90 min to get 20 nm nanotip arrays with an aspect ratio of 13 on the surface of the 6 in. silicon wafer. Figure 3 shows the scanning electron microscopy (SEM) pictures of the silicon nanograss mold by 90-min plasma etching. From the SEM pictures, it can be seen that the nanocavities are about 40 nm and the small gaps between the silicon nanotips are less than 5 nm. In order to reduce surface energy of the silicon master mold for ease of demolding, trichloro(1*H*,1*H*,2*H*,2*H*-perfluorooctyl)silane(FOTS) was deposited on the silicon surface at 250 °C for 2 h by chemical vapor deposition techniques. After the process, the silicon master mold was washed using hexane. The self-assembled monolayer, having a very low surface energy due to its CF groups, was applied on the silicon surface. The contact angel of the FOTS-coated silicon nanograss surface is 158°. This study uses Topas COC 6015 plastic, with a glass temperature (T_g) of 150 °C. Four inch COC blank wafers were prepared by injection molding. The silicon nanograss mold was used for nanoimprinting COC surfaces with molding temperatures ranging from 120 °C (below T_g) to 220 °C (above T_g). Nanoimprinting was performed at a fixed pressure and fixed process duration by a hot-embossing machine. The hot embossing equipment used was a hydraulic hot-press machine consisting of a heating and pressing component. The heating component produced heat through a heating coil which was evenly distributed to the pressing component through a heat spreader with the PID controller to regulate the set temperature. The pressing component used hydraulic jacks to exert forces and was connected to a pressure gauge that measured the forces. Before each hot press, all specimens and materials were prewashed twice with methanol and DI water, and then a high-pressure nitrogen gun was used to blow away the residual liquid to complete the cleaning treatment. First, a stack of silicon mold and blank COC wafer were heated to specific molding temperature. While the specimen was evenly heated, an initial pressure of 0.1 MPa was applied to the wafers surface to evenly transmit the heat to the wafers. This initial process lasted for 5 min until reaching a steady temperature. Once the wafer temperature reached the specified level, it was molded using the polymer microstructure hot-press by applying hot-press pressure of 1 MPa onto the COC wafer and the silicon mold through the hydraulic rod, extruding the molten polymer material to fill the nanocavities in the mold. Both the temperature and pressure were maintained at a fixed level, and after 15 min the thermal nanoimprinting was complete. After molding, the temperature switch was turned off to allow the temperature to cool slowly to below the polymer material glass transition temperature of 40 °C (below the heat distortion temperature). So, the pressure was maintained until the COC was cooled down to 110 °C. According to the experiments, the polymer nanostructures nanoimprinted below 150 °C are self-detached from the silicon master mold. The nanostructures nanoimprinted between 150 and 180 °C are easy to be demolded with assist of small force on edge of the chips. The nanostructures nanoimprinted above 180 °C are difficult to be demolded. The nanostructures nanoimprinted above 180 °C were obtained by etching away the silicon mold with 10% Tetramethylammonium Hydroxide (TMAH) solution. According to our testing, blank COC polymer can survive in 10% TMAH solution without damage on the polymer surface. COC chips with different HAR nanostructural morphologies were fabricated using thermal nanoimprint techniques. In addition, silicon master molds have been investigated by SEM images after the demolding process to show no damage on the silicon nanograss structures.

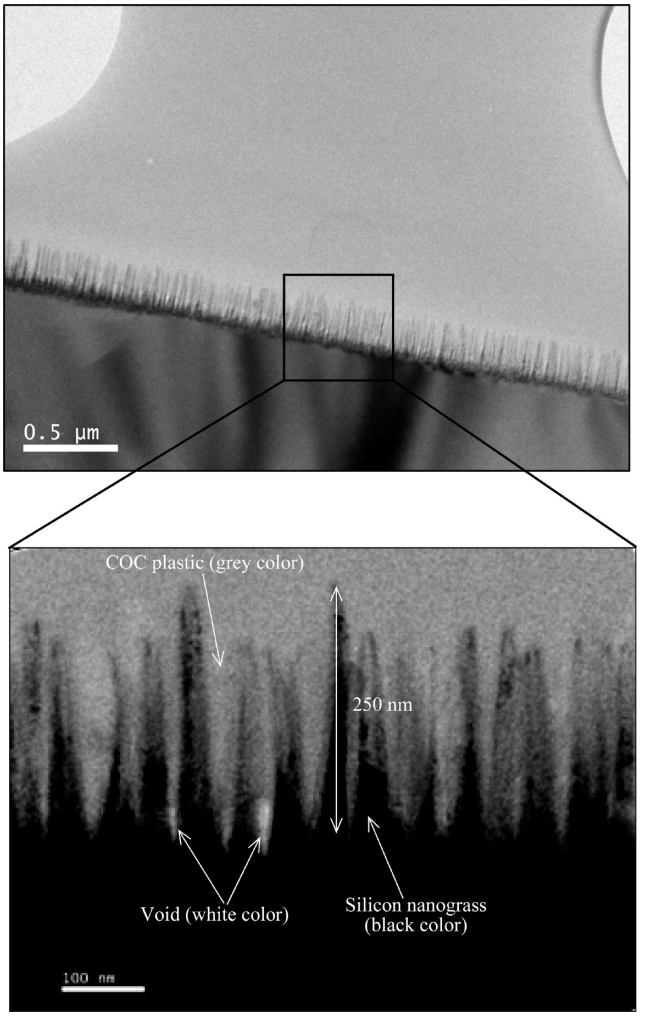

Figure 4. TEM pictures of the nanoimprinted sub-20-nm COC polymer nanotips with 180 °C molding temperature before the demolding process.

Results and Discussion

The transmission electron microscopy (TEM) pictures (cross section) of the nanoimprinted sub-20-nm COC polymer nanotips with 180 °C molding temperature before demolding process are shown in Figure 4. Sub-20 nm nanotip arrays were formed on the plastic surface before scanning electron microscopy imaging. The pictures also show that COC plastic has been successfully imprinted with silicon mold with no damage of silicon nanograss structures. COC plastic surfaces after nanoimprinting are pictured by

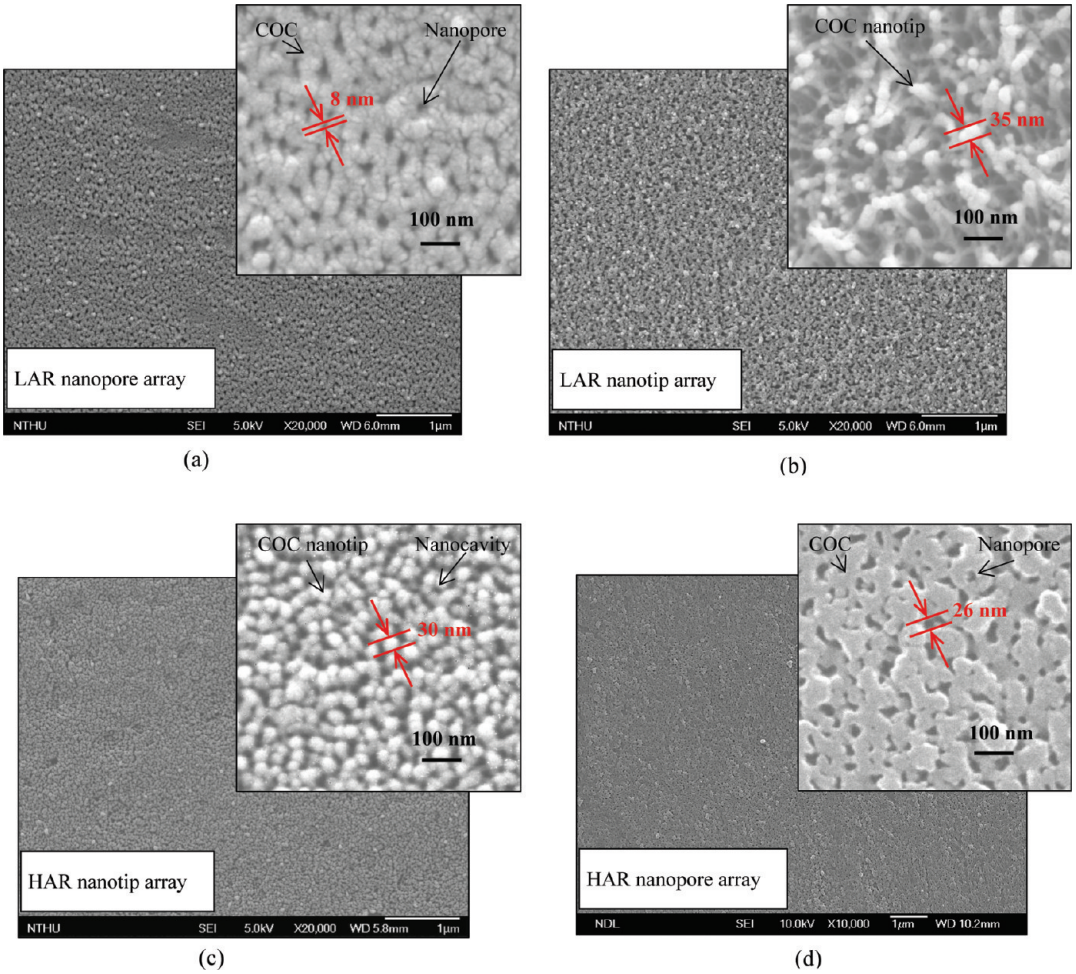

Figure 5. SEM pictures of top view of the nanoimprinted sub-20-nm COC polymer nanotip and nanopore arrays with different molding temperatures: (a) 120 °C; (b)160 °C; (c)180 °C; (d) 220 °C. The inset images are high-magnification top view of the structure, respectively.

SEM, shown in Figure 5. Platinum layers with a thickness of 9 nm were deposited onto the surface of the samples before SEM imaging. The SEM pictures of top view of the nanoimprinted sub-20-nm polymer nanotips with a molding temperature of 120 °C are shown in Figure 5a. The polymer surface is heated to be softened while it is heated up to the specific temperature, so the silicon nanotips slightly penetrate into the polymer surface. Low-aspect-ratio (LAR) nanopore arrays are formed on the COC plastic surfaces at this stage. When the molding temperature was increased to 160 °C, the COC nanotips were slightly deformed during the demolding process due to the mismatch of the thermal expansion between COC and silicon, shown in Figure 5b. The SEM pictures of top view of the nanoimprinted sub-20-nm polymer nanopores with a molding temperature of 180 °C are shown in Figure 5c. From this result, it can be seen that high-aspect-ratio (HAR) nanoimprinted plastic nanotips are surrounded by air. The SEM pictures of top view of the nanoimprinted sub-20-nm polymer nanopores with a molding temperature of 220 °C are shown in Figure 5d. Found from the result, it can be seen clearly that plastic flow completely filled the nanocavities of the silicon mold to form high-aspect-ratio nanopore arrays. It is found that different morphologies of polymer nanostructures from nanopores to nanotips can be easily fabricated using the identical mold structure just by adjusting the molding temperatures.

After nanoimprinting, nano microstructures with diameters of 20 nm form on the surface of polymer materials, changing their optical and surface properties such as transmittance, contact angel characteristics. Water contact angle measurements are used to represent surface hydrophobicity. A droplet of 2.5 μL D.I. water was deposited on the COC polymer surface by a micro pipet for the contact angle measurement. No additional chemical coating is needed to modify COC from a native contact angel of 90° into a hydrophobic (100−155°). Surface properties were changed with different molding temperature (nanostructural morphologies), as shown in Figure 6. While the morphologies of the nanostructures are changed from nanopores to nanotips, the air ratios on the polymer surfaces are increased. Obviously, the polymer nanostructured surfaces become more hydrophobic when the contact area of droplets with COC nanostructures is reduced. The Cassie model is often used to explain the relationship between the surface state and structural morphologies. According to the Cassie model, air could trap in the nanocavities around the nanotip structures. Only the top surface area of the nanotips contacts with the droplet. So, air pockets are created underneath the droplet. On the basis of the equation of the Cassie model, the structural fraction of the top surface area of the nanotip structures is related to the contact angle of the droplets. When the structural fraction is reduced, the air amount between the droplets and the chip surfaces is increased. Then it will increase the hydrophhobicity of the chip surfaces due the increment air amount between the droplets and the chip surfaces. Experimental results show that the contact angles of the polymer surfaces change with molding temperatures, which are the key factor for controlling nanostructural morphology using thermal nanoimprinting. The optical transmittance of COC chips has been characterized using a conventional UV−vis spectrophotometer (maker, JASCO; model, V-630, double-beam spectrophotometer with single monochromator). The optical transmittance of

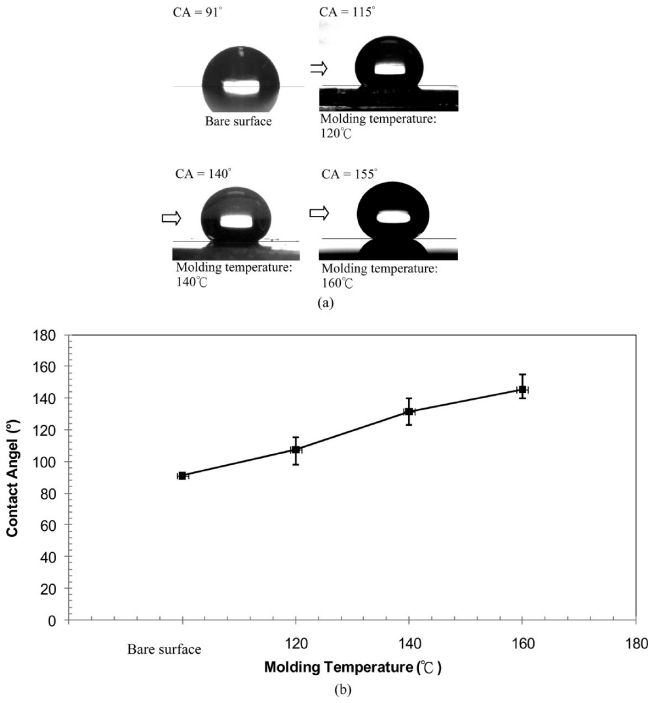

Figure 6. Contact angle measurement results of nanotip and nanopore arrays fabricated with different molding temperatures: (a) photographs of water droplets on the nanostructured COC chips; (b) plot of the measured results.

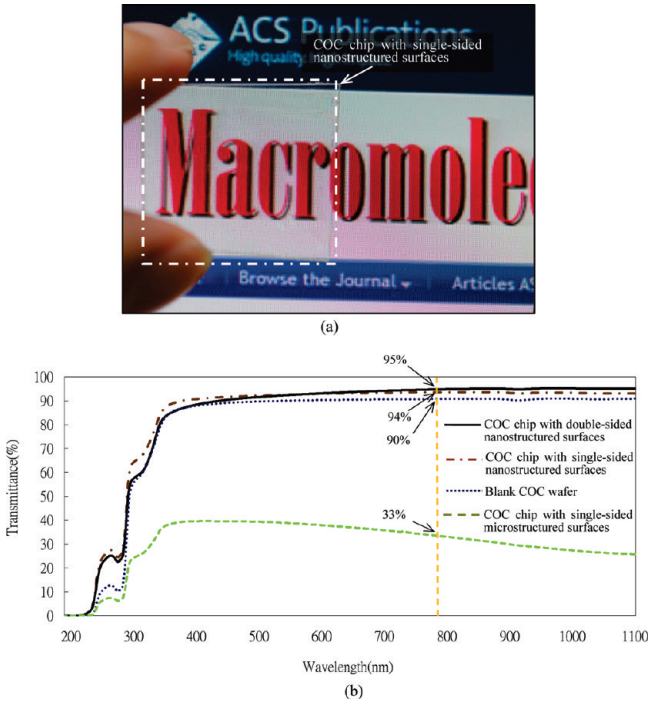

Figure 7. Optical transmittance results: (a) photograph of COC chip with single-sided nanostructured surfaces of COC chips over a LCD screen; (b) optical transmittance of COC chips with different surface treatments.

COC with nanoimprinted surfaces was changed with surface morphologies. The optical transmittance was increased by one layer of HAR nanostructures without any addition chemical coating. The results show that the optical transmittance of COC with different aspect-ratio sub-20-nm nanostructured surface, shown in Figure 7. Found from the results, polymers with microstructured surfaces show a big decrease in optical transmittance. The arrays of the tested microstructures are 15 μm × 15 μm × 2 μm and 8 μm spacing between the microstructures. However, polymer surfaces with aligned HAR nanotip arrays improve optical property due to their structural features, which reduce light reflection. In addition, the optical transmittance of the COC chip with double-sided nanostructured surfaces increased from 90% to 95% in the visible wavelength range. Reflection can be reduced due to the small gradient of the refractive index in the nanostructures region. Because of the reduction of the reflection from the polymer surface, the transmittance of the polymer chips was increased.

Conclusion

Morphology-controlled sub-20-nm polymer nanotip and nanopore arrays have been realized on COC plastic using the identical silicon mold structure by varying molding temperatures of the thermal nanoimprinting process. Sub-20 nm polymer nanostructures with different morphologies can be realized by varying molding temperatures. In addition, they have been investigated the optical and surface properties. Polymers with aligned HAR nanostructured surfaces reduce surface energy. Nanotip or nanopore arrays also increase the ratio of surrounding air between the droplet and polymer substrate, changing the surface properties. COC plastic can be modified to superhydrophobic surface by thermal nanoimprinting process without any chemical treatment. We have been successfully developed a novel and simple technique to modify a COC plastic into a hydrophobic and surperhydrophobic surface by changing the surface morphologies. No additional chemical coating is needed to modify COC from the native contact angle of 90° into a hydrophobic (100−155°). Polymer surfaces with aligned HAR nanotip arrays improve optical property due to their structural features, which reduce light reflection. In addition, the optical transmittance of the COC chip with double-sided nanostructured surfaces increased from 90% to 95% in the visible wavelength range. The study advantageously makes nanotip and nanopore arrays with aspect ratios up to 13 and provides stable superhydrophobicity and high transparency on plastic surfaces. The developed technique is simple, ease of fabrication and low cost to realize morphology-controlled sub-20-nm nanotip and nanopore arrays using the identical silicon mold structure by varying molding temperatures of the thermal nanoimprinting process.

Acknowledgment. This research was supported partially by the National Science Council of Taiwan (NSC 96-2221-E-007-134, NSC 97-2221-E-492-002). We thank Y. C. Chen for help with the silicon nanograss fabrication.

References and Notes

(1) Wang, X.; Berggren, M.; Inganas, O. *Langmuir* **2008**, *24*, 5942–5948.
(2) Roca-Cusachs, P.; Rico, F.; Martínez, E.; Toset, J.; Farre, R.; Navajas, D. *Langmuir* **2005**, *21*, 5542–5548.
(3) Jeong, H. E.; Lee, S. H.; Kim, P.; Suh, K. Y. *Colloids Surf., A* **2008**, *313−314*, 359–364.
(4) Aryal, M.; Buyukserin, F. *J. Vac. Sc., Technol. B* **2008**, *26*, 2562–2566.
(5) Krishnamoorthy, S.; Gerbig, Y.; Hibert, C.; Pugin, R.; Hinderling, C.; Brugger, J.; Heinzelmann, H. *Nanotechnology* **2008**, *19*, 285301–285306.
(6) Zhang, Y.; Lo, C.-W.; Taylor, J. A.; Yang, S. *Langmuir* **2006**, *22*, 8595–8601.
(7) Ebbesen, T. W.; Lezec, H. J.; Hiura, H.; Bennett, J. W.; Ghaemi, H. F.; Thio, T. *Nature* **1996**, *382*, 54–56.
(8) Cheng, T. C.; Shieh, J.; Huang, W. J.; Yang, M. C.; Cheng, M. H. *Appl. Phys. Lett*. **2006**, *88*, 263118–263120.
(9) Tao, A.; Kim, F.; Hess, C.; Goldberger, J.; He, R.; Sun, Y.; Xia, Y.; Yang, P. *Nano Lett*. **2003**, *3*, 1229–1233.
(10) Genet, C.; Ebbesen, T. W. *Nature* **2007**, *445*, 39–46.

(11) Carpenter, J.; Khang, D.; Webser, T. J. *Nanotechnology* **2008**, *19*, 505103–505110.
(12) Ren, H.-X.; Chen, X.; Huang, X.-J.; Im, M.; Kim, D.-H.; Lee, J.-H.; Yoon, J.-B.; Gu, N.; Liu, J.-H.; Choi, Y.-K. *Lab Chip* **2009**, *9*, 2140–2144.
(13) Chunder, A.; Etcheverry, K.; Londe, G.; Cho, H. J.; Zhai, L. *Colloids Surf., A* **2009**, *333* (1−3), 187–193.
(14) Jokinen, V.; Sainiemi, L.; Franssila, S. *Adv. Mater.* **2008**, *20*, 3453–3456.
(15) Erbil, H. Y.; Demirel, A. L.; Avc, Y.; Mert, O. *Science* **2003**, *299*, 1377–1380.
(16) Teshima, K.; Sugimura, H.; Inoue, Y.; Takai, O.; Takano, A. *Langmuir* **2003**, *19*, 10624–10627.
(17) Feng, L.; Zhang, Y.; Xi, J.; Zhu, Y.; Wang, N.; Xia, F.; Jiang, L. *Langmuir* **2008**, *24*, 4114–4119.
(18) Wu, X.; Shi, G. *Nanotechnology* **2005**, *16*, 2056–2060.
(19) Nosonovsky, M.; Bhushan, B. *Nano Lett.* **2007**, *7*, 2633–2637.
(20) Han, D.; Steckl, A. J. *Langmuir* **2009**, *25*, 9454–9462.
(21) Luo, C.; Zuo, X.; Wang, L.; Wang, E.; Song, S.; Wang, J.; Wang, J.; Fan, C.; Cao, Y. *Nano Lett.* **2008**, *8*, 4454–4458.
(22) Chang, K.-C.; Chen, Y.-K.; Chen, H. *Surf. Coatings Technol.* **2008**, *202*, 3822–3831.
(23) Ling, X. Y.; Phang, I. Y.; Vancso, G. J.; Huskens, J.; Reinhoudt, D. N. *Langmuir* **2009**, *25*, 3260–3263.
(24) Vourdas, N.; Tserepe, A.; Gogolides, E. *Nanotechnolgy* **2007**, *18*, 125304–125310.
(25) Shieh, J.; Lin, C. H.; Yang, M. C. *J. Phys. D: Appl. Phys.* **2007**, *40*, 2242–2246.
(26) Shieh, J.; Hou, F. J.; Chen, Y. C.; Chen, H. M.; Yang, S. P.; Cheng, C. C.; Chen, H. L. *Adv. Mater.* **2010**, *22*, 597–601.
(27) Thurn-Albrecht, T.; Schotter, J.; Kästle, G. A.; Emley, N.; Shibauchi, T.; Krusin-Elbaum, L.; Guarini, K.; Black, C. T.; Tuominen, M. T.; Russell, T. P. *Science* **2000**, *290*, 2126–2129.
(28) Kline, R. J.; McGehee, M. D.; Kadnikova, E. N.; Liu, J.; Fréchet, J. M. J.; Toney, M. F. *Macromolecules* **2005**, *38*, 3312–3319.
(29) Botiz, I.; Darling, S. B. *Macromolecules* **2009**, *42*, 8211–8217.
(30) Park, H. J.; Kang, M.-G.; Guo, L. J. *ACS Nano* **2009**, *3*, 2601–2608.
(31) Hua, F.; Sun, Y.; Gaur, A.; Meitl, M. A.; Bilhaut, L.; Rotkina, L.; Wang, J.; Geil, P.; Shim, M.; Rogers, J. A. *Nano Lett.* **2004**, *4*, 2467–2471.
(32) Li, Z.; Gu, Y.; Wang, L.; Ge, H.; Wu, W.; Xia, Q.; Yuan, C.; Chen, Y.; Cui, B.; Williams, R. S. *Nano Lett.* **2009**, *9*, 2306–2310.
(33) Yang, M.-C.; Shieh, J.; Hsu, C.-C.; Cheng, T.-C. *Electrochem. Solid-State Lett.* **2007**, *8*, 131–133.